Mansoura University
Faculty of Engineering
Mansoura Engineering Journal

Theoretical Study of Mixed Convection Cooling of Microprocessor Using CuO Nanofluid

M. M. El-Khouly*, *G. I. Sultan* and M. A. ElBouz

KEYWORDS:

Thermal management; nanofluids; CFD; electronics cooling; microprocessor

***Abstract*— Cooling of electronic equipments is playing an important role in the last decades as a world experiences a technological boom in all fields. In this study, a numerical study for mixed convection cooling of microprocessor is investigated by the use of pure water and CuO-water nanofluid at six different volume concentrations. The model is built, meshed and simulated by Ansys Fluent Package 16.0 and a mesh independence test is carried out. The study is performed by changing heat load (115W, 130W), inlet velocity, at different concentrations of nanofluids (Pure water, 0.5%, 0.86%, 1.5%, 2.25%, 3.5%, 5%). The present results showed that using CuO-water nanofluids over pure water provides an enhancement in heat transfer characteristics. The dimensionless parameters such as Nusselt number, Archimedes number, Prandtl number, friction factor and dimensionless temperature are studied and correlated. An enhancement of 36.5% in thermal hydraulic performance is found at 0.50% volume fraction at Re = 1679.212. The data are correlated with maximum error of 4.1%.**

I. INTRODUCTION

NANOFLUIDS are regarded for a next heat transfer medium, because of their great thermal performance. While technology advanced and electrical equipment became smaller, liquids coolants were frequently utilized in personal computers, notebooks, data centers, and quantum computers. Micro heat sinks are commonly used to improve cooling process using Nanofluids are very important due to their thermal behavior.

Zhang et al. [1] carried out a review for heat transfer options of electronic equipments and highlighted the opportunity of Cellulose Nanofiber-based constituents for effective thermal performance in expressions of energy storage with super capacitors, batteries, and solar panels. Wang et al. [2] presented a literature survey to study the possibility of improving heat transfer characteristics of nanofluids, chaos convection, and heat transfer optimization of nanofluids with the response to an applied electromagnetic field. Alihosseini et al. [3] focused mostly on studying discrepancy in a cross-section effect on the thermal properties efficiency of micro channel heat sinks. Wong et al. [4] provided a broad review of experimental and numerical studies for different styles of thermal diodes applied in past years. The thermal diodes mentioned there were categorized based on their main heat transfer procedure and the constituents to create them. Xu et al. [5] investigated air cooling restrictions for a high power CPU (Central Processing Unit) with high local power density discovered through a thermal model. The thermal model involved a 0.02 m × 0.02 m die with such output power of 160W and a power generation capability of 100W/cm^2 considered. The liquid cooling system volume is 100 mm (flow length) × 100 mm (width) × 45 mm (height), and the shipment area is believed to be 50 mm × 50 mm. Heat transfer and pressure

Received: (17 April, 2021) - Revised: (22 May, 2021) - Accepted: (31 May, 2021)

**** Corresponding Author:** M. M. El-Khouly, Mechanical Power Engineer (e-mail: mohamedmohsenelkhouly@gmail.com).*

G. I. Sultan is with the Mechanical Power Engineering Department, University of Mansoura, CO 35516, Egypt (e-mail: gisultan@mans.edu.eg)

M. A. ElBouz, is with the Mechanical Power Engineering Department, University of Mansoura, CO 35516, Egypt (e-mail: mostafa_booz@yahoo.com)..

(Ser. NO. BFEMU-2104-1110)

Nomenclature

A	Surface area [m^2]
Ar	Archimedes number [-]
C_p	Specific heat [W/(m^2.K)]
f	Friction factor
Gr	Grashof number [-]
$\bar{h}$	Heat transfer coefficient [W/(m^2.K)]
k	Thermal conductivity [W/(m.K)]
L	Heat source length
$\dot{m}$	Mass flow rate [kg/s]
Nu	Nusselt number [-]
p	Static pressure [N/m^2]
Pr	Prandtl number [-]
$\dot{Q}$	Heat transfer rate [W]
Re	Reynolds number [-]
T	Temperature [ºC]
U	Velocity [m/s]
$\vec{v}$	Velocity vector [m/s]

Greek symbols

θ	Dimensionless temperature
μ	Dynamic viscosity [Pa.s]
ν	Air kinematic viscosity [m^2/s]
ρ	Fluid density [kg/m^3]
$\emptyset$	Volume fraction

Subscripts

avg	Average
bf	base fluid
f	Fluid
hs	heat source
i	inlet
max	Maximum
min	Minimum
nf	Nanofluid
o	outlet
s	solid particles
w	Wall

Abbreviations

3-D	Three-Dimensional
CFD	Computational Fluid Dynamics
CNF	Cellulose Nanofiber
CPU	Central Processing Unit
FHP	Flat Plate Heat Pipe
MoS_2	Molybdenum disulfide
MQL	Minimum Quantity Lubrication
	NEPCM Nanoparticle-Enhanced Phase Change Materials
PCM	Phase Change Materials
PLMC	Pumped Liquid Multiphase Cooling
PV	Photovoltaic
PVT	Photovoltaic Thermal
RT-35HC	A commercial-grade of paraffin

loss are predicted using statistical tactics. Finally, the outputs of the numerical investigation and heat sink efficiency are used to predict air flow. Hannemann et al. [6] characterized the fundamental pumped liquid multiphase cooling (PLMC) technique and current experimental outcomes from various prototype implementations of the technique. Schmidt [7] investigated the capacity and package design, as well as additional cooling systems besides air. Several aspects were debated, as well as two sole IBM database packages and the cooling technique they developed. Phan et al. [8] summarized latest progresses during their research of the preparation, optimization, and features of carbon-nanotube-based liquids, such as nano particles, nano-lubricants, and several types of nanofluids enclosing multi-walled carbon nanotubes/single-walled carbon nanotubes/graphene. Kumar et al. [9] carried out a review and explanation of phase change material and Nanoparticle-enhanced phase change materials (NEPCM) combined PVT (Photovoltaic thermal) configurations. Also explained were the several techniques of preparation NEPCM and its thermo-physical characteristics at various operational temperatures for specific applications, the use of nanoparticles, phase change material, and NEPCM in extracting thermal energy from commonly produced PVT systems, and the efforts made by scientists all over the world to enhance the heat transfer performance management system. Nourbakhsh et al. [10] explored the influence of radiation and magnetohydrodynamics on energy transfer of a nanofluid flow over a surface at constant wall temperature or heat capacity. The influences of magnetohydrodynamics and radiation on the surface were believed to be uniformly, and the surface was considered to be motionless. They found that increasing in magnetohydrodynamic parameters lead to increased fluid surface penetration near the surface. The temperature difference increased with the radiation parameter, causing the fluid velocity to rise. Esfe et al. [11] examined experimentally the impact of adding MgO nanoparticles to water mostly on turbulent flow thermophysical behavior of a counter-flow heat exchanger. Studies were conducted out with Reynolds numbers ranging from 6,000 to 32,000 and nanomaterials volume fractions ranging from 0.005 to 0.02. The heat transfer coefficient, pressure loss, friction coefficient, and Nusselt number are all calculated and studied. He et al. [12] investigated thermal improvement techniques in various structural micro heat sinks. Furthermore, non-uniform surface temperature, that included rise in temperature along its streamlines, and hotspots, particularly spontaneous hotspots with high heat flux, were major problems in the thermal utilization of electronic equipment. Existing thermal improvement techniques in micro heat sinks and the decrease of non-uniform temperature profile were adopted. Finally, the obstacles and difficulties for the advancement of thermal utilization of electronic equipment using micro heat sinks

were examined. Brahim and Jemni [13] used COMSOL Multiphysics to mathematically study a 3-D FHPs (Three-Dimensional Flat Plate Heat Pipe) with multiple heating systems. The feasibility of using copper metal powder as a wick structure was explored. The amount of heat flux and hotspot locations on heat pipe efficiency was investigated. The findings revealed that the top hot spot positions, mainly those closest to the walls, have been the most susceptible to dry out. The sizes of hot spots, and also their lengths and pore size diameter, all had a substantial impact on heat pipe performance. Hassan et al. [14] studied the experimental methodology tested outdoors in Taxila, Pakistan to lower PV (Photovoltaic) temperature with the simultaneous use of nanofluid (graphene/water) and phase change material (RT-35HC). Performance of this hybrid PVT system in terms of PV temperature, electric efficiency, thermal efficiency and overall efficiency, was compared with PVT/PCM (Phase Change Materials) system integrated with water flowing through tubes inside PCM, PV/PCM system and conventional PV. Baslem et al. [15] investigated 3 types of water-based nanoliquids holding Tio_2, Al_2O_3, and Cu nanoparticles. The Runge-Kutta-Fehlberg technique was used to calculate energy equation numerically. It was discovered that Cu-water nanoliquid improves heat and mass transfer from fin surface. Gaurav et al. [16] performed a case study on jojoba, a vegetable oil, as a candidate oil mixed with or without molybdenum disulfide nano-particles ($nMoS_2$) in difficult with minimal lubricating oil (MQL). For machining Ti-6Al-4V alloy, jojoba oil was compared to commercially available mineral oil (LRT 30). Cutting force, surface roughness, and tool wear were reduced by 35-47 percent when MQL spinning with jojoba oil + $nMoS_2$ (0.1 percent). Furthermore, the findings demonstrated that jojoba oil, and also jojoba oil with an optimal concentration of MoS_2 nanoparticles, started to emerge as a viable machining option. Mukesh Kumar and Arun Kumar [17] calculated the rate of heat transfer, temperature rise, Nusselt number, thermal resistance, power output, and accuracy of a ship in a six-channel heat source using water and Al_2O_3/water nanofluids as coolants. The ANSYS (v12) Fluent software was used to analyze the effectiveness of an electronic chip. The Al_2O_3/water nanofluids were found to reduce the temperature rise, power usage, and thermal resistance of electronic chips more than water. Ali [18] analyzed the heat transfer improvement by perforation in air cooling of 2-in-line rectangular heat generators modules experimentally. At *s/L* = 0.5 and 1.0, two separation lengths between both the heating systems are analyzed. In both scenarios, the area between both the heaters was perforated in an alignment pattern, resulting in holes open space ratios (*b*) of 0, 0.0736, 0.1472, and 0.2944. From previous works, it is clear that using of nanofluids in cooling processes are very valuable point of interest especially for cooling of microprocessor due to large usage of it at last decades.

II. AIM OF THE PRESENT WORK

The aim of this analysis is displaying the effect of using nanofluids at various concentrations for cooling of electronic components overusing water or air as a coolant. We will study the cooling of microprocessors for water as a base fluid and CuO nanoparticles suspended in water at various concentrations of (0.5, 0.86, 1.5, 2.25, 3.5, and 5%). A numerical study is carried out for water and nanofluid. The heat transfer coefficient, Nusselt number, friction factor, Archimedes number and thermal hydraulic performance at different Reynolds numbers are predicted.

III. CHARACTERISTICS OF CUO-WATER NANOFLUID

The thermophysical properties of the nanofluid are estimated as follows [19]:

$$\rho_{nf} = \emptyset\, \rho_p + (1-\emptyset)\rho_{bf} \quad (1)$$

$$Cp_{nf} = \frac{\emptyset \rho_p Cp_p + (1-\emptyset)\rho_{bf} Cp_{bf}}{\rho_{nf}} \quad (2)$$

$$\mu_{nf} = \mu_{bf}(1 + 2.5\,\phi) \quad (3)$$

$$\frac{k_{nf}}{k_{bf}} = \left(\frac{k_s}{k_{bf}}\right)^{\phi} \quad (4)$$

The surface area of the heat source is given by:

$$A_{h,s} = L_1 * L_2 + 4 * (L_2 * h) \quad (5)$$

where $A_{h,s}$ is the surface area of heat source, m^2, L_1: length of the outside wall, L_2: length of the heater, and *h*: height of the heater.

The average heat transfer coefficient from the heater to the liquid passing in the heat sink is given by [20]:

$$\bar{h} = \frac{\dot{Q}}{A_{h,s}\left(T_{w,avg} - T_b\right)} \quad (6)$$

where; T_b is the bulk cooling water temperature, $(T_i + T_o)/2$, and $A_{h,s}$ is the surface area of the heat source. The flow rate of nanofluid is calculated as:

$$\dot{m}_{nf} = \frac{\rho_{nf} V_{nf}}{\tau} \quad (7)$$

$$\dot{u}_m = \frac{\dot{m}_{nf}}{\rho_{nf} A_c} \quad (8)$$

where A_c is the cross-section area of fluid flow around heater.

$$A_c = L_1 H - L_2 h \quad (9)$$

h: height of the case.

The Reynolds number is calculated based on the heat sink volumetric hydraulic diameter as:

$$\mathrm{Re_D} = \frac{\rho_{nf}\ u_m\ D}{\mu_{nf}} \quad (10)$$

$$D = \frac{4V}{A} \quad (11)$$

Where *D*: Volumertic hydraulic diameter.

V: The enclosed (wetted) volume.

A: Surface area within that flow length [21].

The Nusselt number, dimensionless temperature, Archimedes number, friction factor and thermal hydraulic performance are calculated from the following equations:

$$N_u = \frac{h \times L}{k} \quad (12)$$

$$\theta = \frac{T_{avg} - T_f}{qL/k_f} \quad (13)$$

$$Ar = \frac{Gr}{Re^2} \quad (14)$$

$$Pr = \frac{\mu\, C_p}{k} \quad (15)$$

where Gr regards to Grashof number and is calculated from the following equation:

$$Gr = \frac{g \times \beta \times (T_{avg} - T_f) \times L^3}{\vartheta^2} \quad (16)$$

For laminar condition in this study, the friction factor can be calculated as:

$$f = \frac{64}{Re} \quad (17)$$

Finally, thermal hydraulic performance ζ is calculated for optimization of heat transfer characteristics through various volume fractions used in our model as:

$$\zeta = \frac{Nu}{Nu_o} / \left(\frac{\Delta P}{\Delta P_o}\right)^{\frac{1}{3}} \quad (18)$$

IV. Theoretical Analysis

In this section, steady state laminar flow condition is applied for simulating the characteristics of heat transfer and friction of a microchip using nanofluid. The thermophysical properties of a nanofluid are described by the nanofluidic thermal conductivity. The value of $k_s = 76.5 \text{W/(m·K)}$ is adopted to be constant [22]. To estimate the thermophysical properties of the base fluid, temperature dependent properties were used. For water, the value of k_f is calculated using a fourth order polynomial function of temperature and valid for a temperature ranging from 274 to 633 K [23],

$$k_{bf} = -0.432 + 0.0057255 \times T - 8.078 \times 10^{-6} T^2 + 1.861 \times 10^{-9} T^3 \ \frac{W}{Km^{-1}} \quad (19)$$

Different formulas were suggested to measure the nanofluid viscosity. In the study of CFD modeling of nanofluids, the classic Brinkman model [24] seems to have been used widely. In another side, the density and specific heat capacity nanofluids are widely measured by Seyf and Feizbakhshi [25].

TABLE 1
PROPERTIES OF CuO NANOPARTICLES, [25]

Material	Specific heat (kJ/kg K)	Thermal conductivity (W/m K)	Density (kg/m^3)
Copper oxide (CuO)	0.551	33	6000

The computational domain used in the current CFD (Computational Fluid Dynamics) simulation is depicted in Fig. 2. The computational domain was built, meshed, and simulated using ANSYS-Fluent 16.0. The computational domain consists of 1,464,787 elements. This number of elements were obtained after the mesh independence test. More details about the mesh characteristics were presented in Table 2. The span of the inlet and outlet pipe chosen to be five times the diameter of the heater to validate a fully developed flow. The flow is considered laminar flow through the calculations [25], [26].

Continuity equation:

$$\frac{\partial \rho}{\partial t} + \left(\rho \vec{v}\right) = 0 \quad (20)$$

Momentum equation:

$$\frac{\partial \rho \vec{v}}{\partial t} + \nabla . \left(\rho \vec{v} \vec{v}\right) = -\nabla P + (\tau) + \rho \vec{g} \quad (21)$$

where P, τ, and $\rho\vec{g}$ are the pressure, stress tensor and the body force resulted due to the gravity effect. The stress tensor τ is given by:

$$\tau = \mu(\nabla \vec{v} + \nabla \vec{v}^T) - \frac{2}{3}\mu \nabla \vec{v} I \quad (22)$$

The flow energy equation is expressed as follows:

$$\frac{\partial \rho E}{\partial t} + \nabla . (\rho \vec{v} h) = \nabla . (k \nabla T) \quad (23)$$

TABLE 2
MESH INDEPENDENCE TEST

No. of Elements	841,547	904,360	1,105,366	1,225,798	1,464,787	1,595,750
h (W/m^{2}K)	1258.63	1258.95	1259.36	1259.69	1260.41	1260.12

For the boundary condition, at the test section inlet, a uniform normal inlet velocity with uniform inlet temperature is assumed. The speed at the inlet is ranging from 0.075 to 0.145 m/s. Zero (gage) pressure is defined at the test section outlet. Uniform heat flux was attained with a value of 40,000 W/m^2. No slip boundary is used at the walls and the interfaces between the wall and the fluid. ANSYS Fluent 16 is used to simulate the problem. Second order upwind scheme pressure-based solver is applied with SIMPLE algorithm for the pressure-velocity coupling [27]. The solution is performed and modeled, the values were achieved at monitor residuals under 10^{-6} for the momentum and energy equation. In addition, both the inlet pressure and outlet temperatures were controlled as a measure for the convergence criteria.

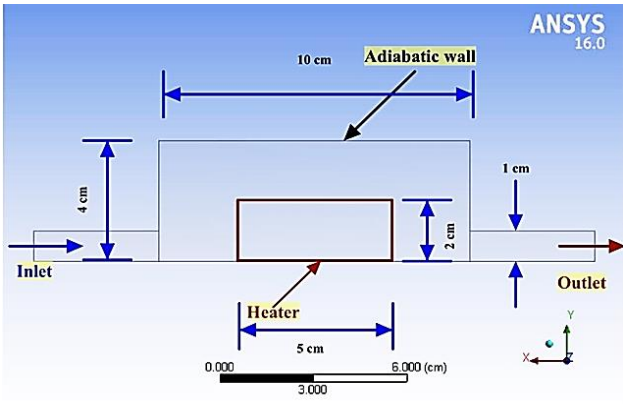

Fig. 1 Geometry of the simulation

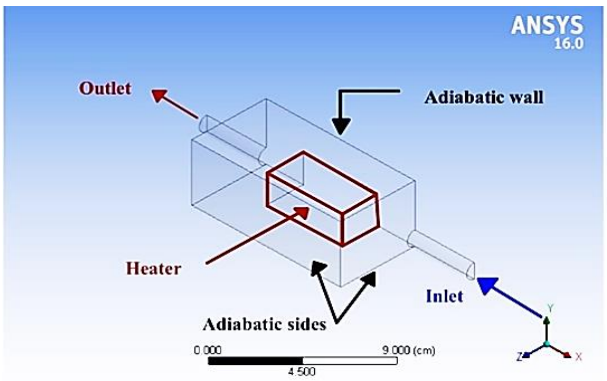

Fig. 2 Half of the model

TABLE 3
MESH DETAILS

Number of elements	1,464,787
Orthogonal quality	
Min	0.22328
Max	1
Average	0.87778
Standard deviation	8.5712e-002
Element quality	
Min	6.3831e-002
Max	1
Average	0.75433
Standard deviation	0.22371

V. RESULTS AND DISCUSSION

Model validation

In the present study, the heat transfer characteristics of CuO-Water nanofluid over pure water for cooling of microprocessors was numerically investigated. Fig. 4 represents the various heat transfer coefficient *h* and Reynolds number *Re* for the present numerical results and the data provided by He et al. [28]. It is clear that there is an agreement with a maximum deviation of about 6.8% between the model and the results obtained by [28]. From Fig. 3, when the Reynolds number *Re* is increased, the heat transfer coefficient *h* is increased.

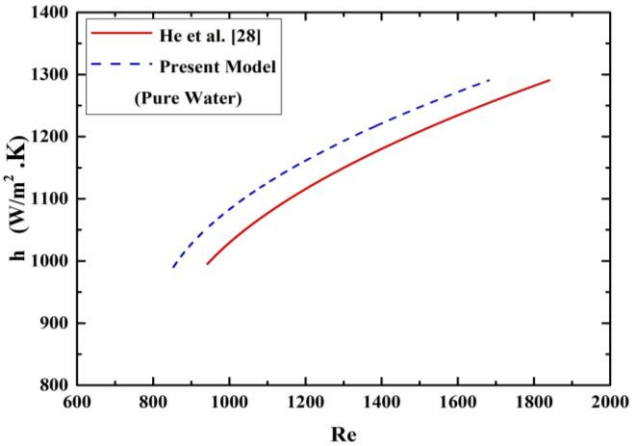

Fig. 3 Validation curve
(Heat transfer coefficient with Reynolds number)

After validating our model, various parameters are studied at different inlet velocities such as, CPU temperature, Nusselt number, dimensionless temperature, Archimedes number and thermal hydraulic performance ζ at different Reynolds numbers. Figure 4 shows the variation between CPU temperature and Reynolds number at various concentrations. A decrease in CPU temperature is observed with increasing the Reynolds number and concentration of CuO nanoparticles due to the enhancement of heat transfer characteristics with using the nanoparticles.

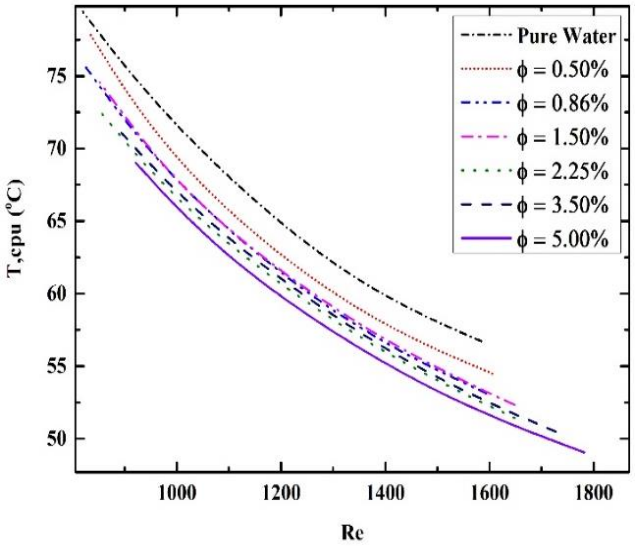

Fig. 4 CPU temperature versus Reynolds number at various concentrations at Q = 130 W

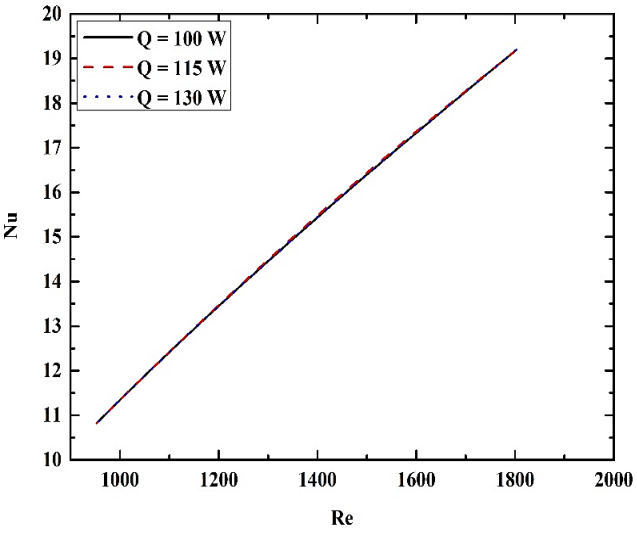

Fig. 5 Nusselt number versus Reynolds number at volume fraction 3.50% at different heat loads

The variation of the Nusselt number with the Reynolds number at different heat loads at Ø = 3.5% is shown in Figure

5. The change of heat loads hadn't a noticeable effect on change of Nusselet number at various Reynolds numbers.

Figure 6 shows the variation between the dimensionless temperature and Reynolds number at different nanoparticles concentrations, the higher volume fraction of 3.50%, 5.00% have higher dimensionless temperature than pure water and the other concentration have less values than pure water and by increasing the Reynolds number, the dimensionless temperature is decreased through all volume fractions.

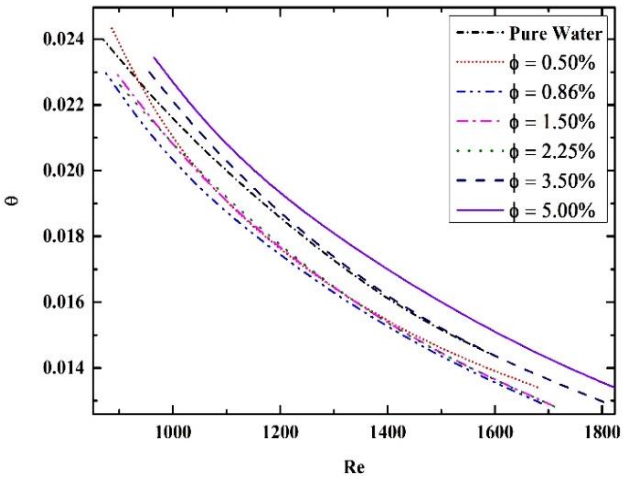

Fig. 6 Dimensionless temperature with Reynolds number at different volume fractions

From Figure 7(A), an increase in Archimedes number is shown with increasing the dimensionless temperature at different concentrations. Otherwise, a decrease in Nusselt number is observed with increasing Archimedes number at different concentrations in Figure 7(B). Although, it is clear that Archimedes number falls in the range from 0.5 to 4 which means a mixed convection dominated flow is existed.

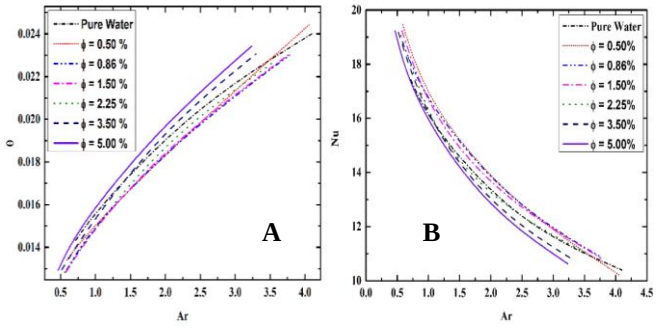

Fig. 7 (A) Archimedes number with dimensionless temperature at various concentrations, (B) Archimedes number with Reynolds number at various concentrations

A friction factor variation with Reynolds number is discussed in Figure 8 at different volume fractions, a decrease in friction factor with increase of Reynolds number is observed at all concentrations in Figure 8.

Figure 9 shows the thermal hydraulic performance with different Reynolds numbers at all nanoparticles concentrations. A thermal hydraulic performance for volume fraction of 5% is observed to be less than 1 in the range $Re < 1500$ and begin to increase at this value which means that the heat transfer enhancement doesn't exist before this value, but it is less than pure water. For $1100 \leq Re \leq 1400$, the thermal hydraulic performance has a decrease in its value in this range for all volume concentrations except for $\emptyset = 0.5\%$ and $\emptyset = 5\%$. The best volume fraction which enhances the heat transfer characteristics through the all cases is $\emptyset = 0.5\%$.

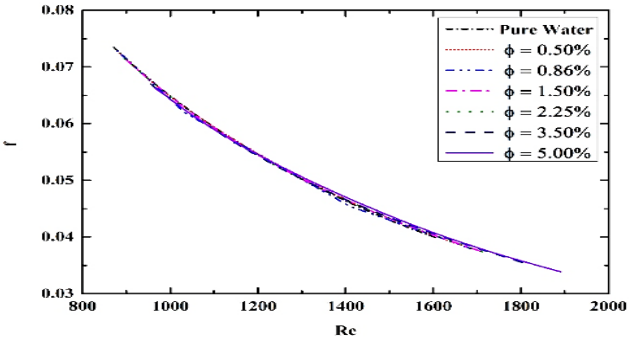

Fig. 8 Friction factor variation with Reynolds number at different volume fractions

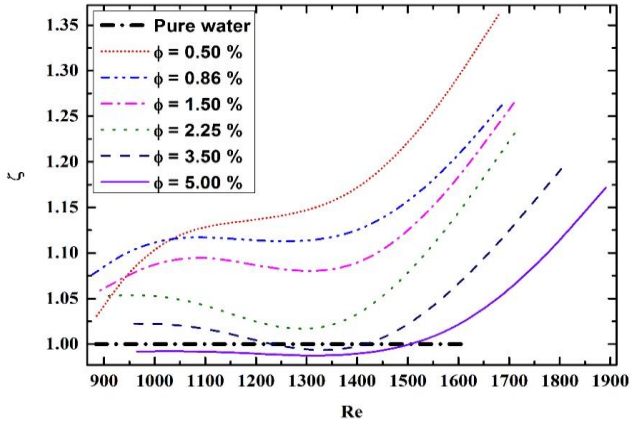

Fig. 9 Thermal hydraulic performance with Reynolds number at different volume fractions

The present results are correlated as:

$$Nu = 0.0265 \times Re^{0.8} \times Pr^{\frac{1}{3}} \times (1-\emptyset)^{0.2738} \quad (24)$$

$$Nu = 16.279 \times Ar^{-0.3} \times (1-\emptyset)^{1.0656} \quad (25)$$

This correlation is valid in the range of operating condition as

$0.4 \leq Ar \leq 4.2$, $0\% \leq \emptyset \leq 5\%$, $800 \leq Re \leq 1900$,
$5.33437 \leq Pr \leq 6.314242$, $10.21796 \leq Nu \leq 19.44556$

The maximum error between the obtained results and the correlated results was observed to be 4.1% as shown in Figure 10.

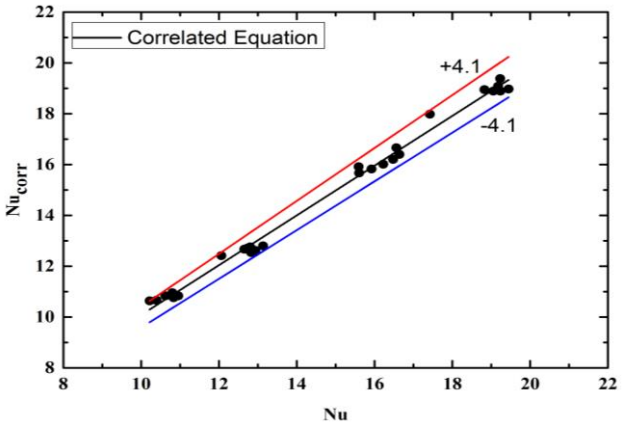

Fig. 10 Correlated Nusselt number versus calculated Nusselt number

VI. CONCLUSION

In this work, the impact of nanoparticles on microchip cooling was evaluated numerically. Water and a CuO–water nanofluid at six different concentrations (0.5, 0.86, 1.5, 2.25, 3.5, and 5 vol. %) were used as cooling liquids. The computational domain was built, meshed, and simulated using the commercial ANSYS Fluent 16 software package. These results confirmed that:

1- The maximum temperature of the processor is decreased by 13.51% at 5.00% volume fraction at *Re* = 1890.748.
2- No noticeable change in Nusselt number at different heat loads examined.
3- A maximum enhancement in non-dimensional temperature of 10.4% is observed at 2.25% volume fraction at *Re* = 1710.822.
4- The maximum enhancement in Nusselt number was observed to be 11.6% at *Re* = 1679.212 of 0.5% volume fraction.
5- Mixed convection dominated flow is observed as Archimedes number falls in the range of 0.5 and 4.
6- An enhancement of 36.5% in thermal hydraulic performance is found at 0.50% volume fraction at *Re* = 1679.212.
7- The presented data are correlated with maximum error of 4.1% in the range mentioned above.

REFERENCES

[1] Y. Zhang, N. Hao, X. Lin, and S. Nie, "Emerging challenges in the thermal management of cellulose nanofibril-based supercapacitors, lithium-ion batteries and solar cells: A review," *Carbohydr. Polym.*, vol. 234, p. 115888, 2020, doi: 10.1016/j.carbpol.2020.115888.

[2] G. Wang, Z. Zhang, R. Wang, and Z. Zhu, "A review on heat transfer of nanofluids by applied electric field or magnetic field," *Nanomaterials*, vol. 10, no. 12, pp. 1–24, 2020, doi: 10.3390/nano10122386.

[3] Y. Alihosseini, M. Z. Targhi, M. M. Heyhat, and N. Ghorbani, "Effect of a micro heat sink geometric design on thermo-hydraulic performance: A review," *Appl. Therm. Eng.*, vol. 170, p. 114974, 2020, doi: 10.1016/j.applthermaleng.2020.114974.

[4] M. Y. Wong, C. Y. Tso, T. C. Ho, and H. H. Lee, "A review of state of the art thermal diodes and their potential applications," *Int. J. Heat Mass Transf.*, vol. 164, 2021, doi: 10.1016/j.ijheatmasstransfer.2020.120607.

[5] G. Xu, B. Guenin, and M. Vogel, "Extension of air cooling for high power processors," *Thermomechanical Phenom. Electron. Syst. - Proceedings Intersoc. Conf.*, vol. 1, no. 858, pp. 186–193, 2004, doi: 10.1109/itherm.2004.1319172.

[6] R. Hannemann, J. Marsala, and M. Pitasi, "Pumped liquid multiphase cooling," *Am. Soc. Mech. Eng. Electron. Photonic Packag. EPP*, vol. 4, pp. 469–473, 2004, doi: 10.1115/IMECE2004-60669.

[7] R. Schmidt, "Challenges in Electronic Cooling - Opportunities for Enhanced Thermal Management Techniques - Microprocessor Liquid Cooled Minichannel Heat Sink," *Heat Transf. Eng.*, vol. 25, no. 3, pp. 3–12, 2004, doi: 10.1080/01457630490279986.

[8] N. M. Phan, H. T. Bui, M. H. Nguyen, and H. K. Phan, "Carbon-nanotube-based liquids: A new class of nanomaterials and their applications," *Adv. Nat. Sci. Nanosci. Nanotechnol.*, vol. 5, no. 1, pp. 3–8, 2014, doi: 10.1088/2043-6262/5/1/015014.

[9] R. R. Kumar, M. Samykano, A. K. Pandey, K. Kadirgama, and V. V. Tyagi, "Phase change materials and nano-enhanced phase change materials for thermal energy storage in photovoltaic thermal systems: A futuristic approach and its technical challenges," *Renew. Sustain. Energy Rev.*, vol. 133, no. April, p. 110341, 2020, doi: 10.1016/j.rser.2020.110341.

[10] A. Nourbakhsh, H. Mombeni, and M. Bayareh, "Effects of radiation and magnetohydrodynamics on heat transfer of nanofluid flow over a plate," *SN Appl. Sci.*, vol. 1, no. 12, pp. 1–8, 2019, doi: 10.1007/s42452-019-1634-6.

[11] M. H. Esfe, A. A. A. Arani, and M. Rezaee, "Experimental thermal analysis of a turbulent nano enriched water flow in a circular tube," *Phys. A Stat. Mech. its Appl.*, p. 124010, 2020, doi: 10.1016/j.physa.2019.124010.

[12] Z. He, Y. Yan, and Z. Zhang, "Thermal management and temperature uniformity enhancement of electronic devices by micro heat sinks: A review," *Energy*, vol. 216, p. 119223, 2021, doi: 10.1016/j.energy.2020.119223.

[13] T. Brahim and A. Jemni, "CFD analysis of hotspots copper metal foam flat heat pipe for electronic cooling applications," *Int. J. Therm. Sci.*, vol. 159, no. December 2019, p. 106583, 2021, doi: 10.1016/j.ijthermalsci.2020.106583.

[14] A. Hassan, A. Wahab, M. A. Qasim, M. M. Janjua, M. A. Ali, H. M. Ali, T. R. Jadoon, E. Ali, A. Raza, and N. Javaid, "Thermal management and uniform temperature regulation of photovoltaic modules using hybrid phase change materials-nanofluids system," *Renew. Energy*, vol. 145, pp. 282–293, 2020, doi: 10.1016/j.renene.2019.05.130.

[15] A. Baslem, G. Sowmya, B. J. Gireesha, B. C. Prasannakumara, M. Rahimi-Gorji, and N. M. Hoang, "Analysis of thermal behavior of a porous fin fully wetted with nanofluids: convection and radiation," *J. Mol. Liq.*, vol. 307, p. 112920, 2020, doi: 10.1016/j.molliq.2020.112920.

[16] G. Gaurav, A. Sharma, G. S. Dangayach, and M. L. Meena, "Assessment of jojoba as a pure and nano-fluid base oil in minimum quantity lubrication (MQL) hard-turning of Ti–6Al–4V: A step towards sustainable machining," *J. Clean. Prod.*, vol. 272, p. 122553, 2020, doi: 10.1016/j.jclepro.2020.122553.

[17] P. C. Mukesh Kumar and C. M. Arun Kumar, "Numerical study on heat transfer performance using Al2O3/water nanofluids in six circular channel heat sink for electronic chip," *Mater. Today Proc.*, vol. 21, part 1, pp. 194–201, 2020, doi: 10.1016/j.matpr.2019.04.220.

[18] R. K. Ali, "Heat transfer enhancement from protruding heat sources using perforated zone between the heat sources," *Appl. Therm. Eng.*, vol. 29, no. 13, pp. 2766–2772, 2009, doi: 10.1016/j.applthermaleng.2009.01.010.

[19] A. Azari, M. Kalbasi, and M. Rahimi, "CFD and experimental investigation on the heat transfer characteristics of alumina nanofluids under the laminar flow regime," *Brazilian J. Chem. Eng.*, vol. 31, no. 2, pp. 469–481, 2014, doi: 10.1590/0104-6632.20140312s00001959.

[20] A. E. Kabeel, G. I. Sultan, Z. A. Zyada, and M. I. El-Hadary, "Performance study of spot cooling of tractor cabinet," *Energy*, vol. 35, no. 4, pp. 1679–1687, 2010, doi: 10.1016/j.energy.2009.12.016.

[21] J. E. Hesselgreaves, R. Law, and D. Reay, *Compact Heat Exchangers: Selection, Design and Operation*. Butterworth-Heinemann, Elsevier, 2017.

[22] Y. J. Hwang, Y. C. Ahn, H. S. Shin, C. G. Lee, G. T. Kim, H. S. Park and J. K. Le, "Investigation on characteristics of thermal conductivity enhancement of nanofluids," *Curr. Appl. Phys.*, vol. 6, no. 6 SPEC. ISS., pp. 1068–1071, 2006, doi: 10.1016/j.cap.2005.07.021.

[23] S. M. S. Murshed and C. A. N. de Castro, "A critical review of traditional and emerging techniques and fluids for electronics cooling,"

Renew. Sustain. Energy Rev., vol. 78, no. February, pp. 821–833, 2017, doi: 10.1016/j.rser.2017.04.112.

[24] A. Kamyar, R. Saidur, and M. Hasanuzzaman, "Application of Computational Fluid Dynamics (CFD) for nanofluids," *Int. J. Heat Mass Transf.*, vol. 55, no. 15–16, pp. 4104–4115, 2012, doi: 10.1016/j.ijheatmasstransfer.2012.03.052.

[25] H. R. Seyf and M. Feizbakhshi, "Computational analysis of nanofluid effects on convective heat transfer enhancement of micro-pin-fin heat sinks," *Int. J. Therm. Sci.*, vol. 58, pp. 168–179, 2012, doi: 10.1016/j.ijthermalsci.2012.02.018.

[26] H. H. El-badrawi, E. S. Hafez, M. Fayad, and A. Shafeek, "Ultrastructure responses of human endometrium to inert and copper IUDs as viewed by scanning electron microscopy.," *Adv. Contracept. Deliv. Syst.*, vol. 1, no. 2, pp. 103–111, 1980.

[27] ANSYS® Academic Research Mechanical, "ANSYS Fluent Theory Guide," *ANSYS Inc., USA*, vol. 15317, no. November, pp. 1–759, 2013, [Online]. Available: http://www.pmt.usp.br/ACADEMIC/martoran/NotasModelosGrad/ANSYS Fluent Theory Guide 15.pdf.

[28] Y. He, Y. Jin, H. Chen, Y. Ding, D. Cang, and H. Lu, "Heat transfer and flow behaviour of aqueous suspensions of TiO2 nanoparticles (nanofluids) flowing upward through a vertical pipe," *Int. J. Heat Mass Transf.*, vol. 50, no. 11–12, pp. 2272–2281, 2007, doi: 10.1016/j.ijheatmasstransfer.2006.10.024.

Title Arabic:

دراسة نظرية للتبريد الحراري المختلط للمعالجات الدقيقة باستخدام مائع نانو أكسيد النحاس

Abstract Arabic:

لعب تبريد الأدوات الإلكترونية دورًا مهمًا في العقود الماضية حيث يشهد العالم طفرة تكنولوجية في جميع المجالات. في هذه الدراسة ، تمت دراسة نظرية للتبريد الحراري المختلط للمعالجات الدقيقة باستخدام الماء النقي وأكسيد النحاس النانوي المختلط بالماء عن طريق ستة تركيزات حجمية مختلفة. تم بناء النموذج والشبكة ومحاكاته بواسطة حزمة البرامج (Ansys, Fluent, 16) ، كما تم عمل اختبار استقلالية الشبكة. أجريت الدراسة عن طريق تغيير الحمل الحراري (115 وات ، 130 وات) ، وسرعة الدخول ، وتركيزات مختلفة من السوائل النانوية (ماء نقي ، 0.5٪ ، 0.86٪ ، 1.5٪ ، 2.25٪ ، 3.5٪ ، 5٪). أظهرت النتائج الحالية أن استخدام السوائل النانوية CuO-water بدلاً من الماء النقي يوفر تحسينًا في خصائص انتقال الحرارة. تم دراسة المتغيرات عديمة الوحدات مثل رقم نسلت ، ورقم أرخميدس ، ورقم براندتل ، ومعامل الاحتكاك ، ودرجة الحرارة عديمة الوحدة ، وربطها ببعضها البعض.